Visualization of crack propagation for assisting double cantilever beam test through mechanoluminescence

Nao Terasaki, Yuki Fujio, Yoshitaro Sakata, Shin Horiuchi & Haruhisa Akiyama

Published online: 20 Feb 2018.

Submit your article to this journal ↗

Article views: 1453

View related articles ↗

View Crossmark data ↗

Visualization of crack propagation for assisting double cantilever beam test through mechanoluminescence

Nao Terasaki[a,b], Yuki Fujio[a], Yoshitaro Sakata[a], Shin Horiuchi[b], and Haruhisa Akiyama[b]

[a]National Institute of Advanced Industrial Science and Technology (AIST), Advanced Manufacturing Research Institute (AMRI), Tosu, Saga, Japan; [b]National Institute of Advanced Industrial Science and Technology (AIST), Adhesion and Interfacial Phenomena Research laboratory (AIRL), Tosu, Saga, Japan

ABSTRACT

Here, a mechanoluminescence-assisted double cantilever beam (DCB) test was proposed and its effectiveness was demonstrated. Based on mechanoluminescence, a crack tip was clearly distinguished and successfully tracked during crack propagation and delamination in the DCB test, which helped overcome the difficulty associated with the conventional DCB test. The crack length could be easily determined and used to evaluate the fracture toughness. In addition, mechanoluminescence sensing using the top image of the DCB specimen provided valuable information on the fracture and adhesive frontline to determine the distribution of fracture toughness and adhesive strength under the surface treatment and adhesion curing conditions in the DCB test.

Introduction

Mechanoluminescent (ML) materials are novel functional ceramic powders that can emit intense light under repeated mechanical stress induced by deformation, friction, or impact, even in the elastic deformation region. [1–3] When dispersedly coated onto a structure, each particle acts as a sensitive mechanical sensor, while the two-dimensional (2D) emission pattern of the whole assembly reflects the dynamical strain/stress distribution [1–11], as shown in Figure 1. ML sensors have been used in practical applications such as bridges [3–7], buildings [3,8], welding points of pipelines [3], hydrogen high-pressure hydrogen vessels [9] for structural health monitoring (SHM), or carbon fiber reinforced plastic (CFRP) [10] and adhesion [11] for sophistication of computer aided engineering (CAE) and damage tolerant design. Thus, the ability of an ML sensor to detect potential destruction such as active cracks, real crack propagation, and mechanically weak points has been successfully demonstrated. In particular, when visualizing crack propagation, a discrepancy was reported within 500 μm between the real crack tip identified using a microscope and the ML point, as shown in Figure 1. [3,7]
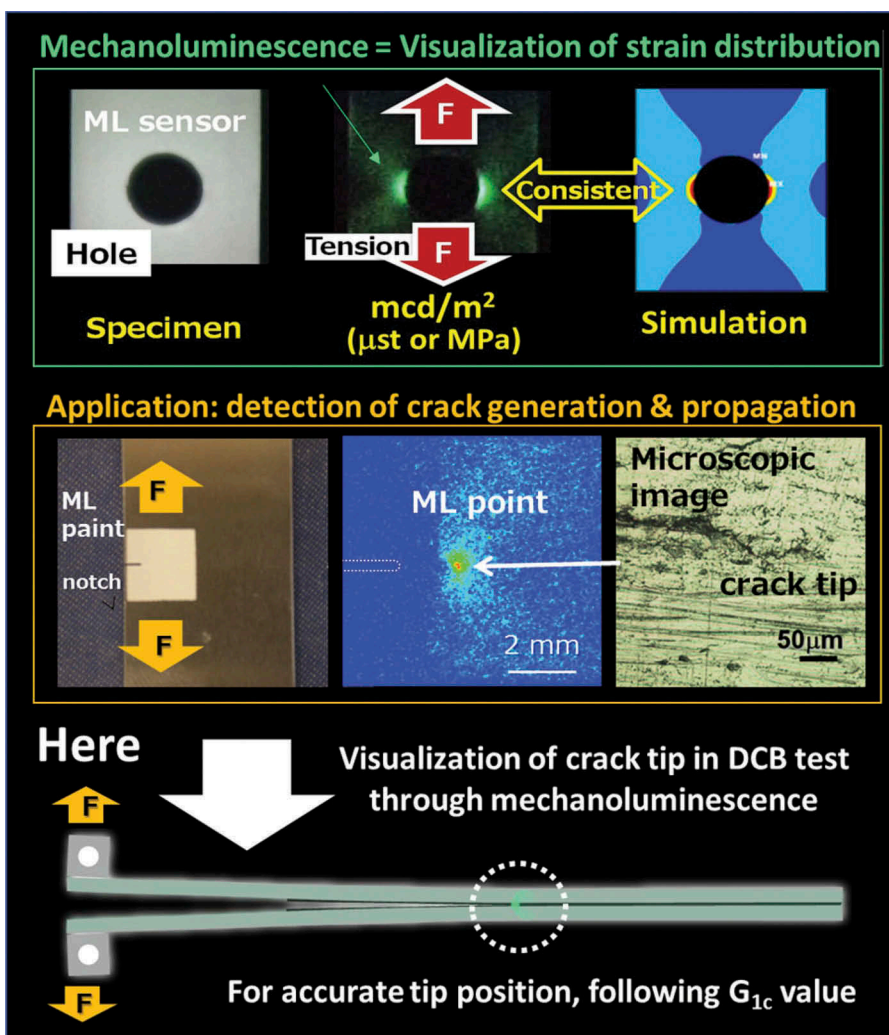
Figure 1. Schematic illustration of feature, application of mechanoluminescence sensing, and concept of mechanoluminescence-assisted DCB test.

The double cantilever beam (DCB) test is one of the most valuable and widely used tools to evaluate the fracture toughness of an adhesive layer. [12–20] Despite its importance, the DCB test involves difficulty in distinguishing the crack tip during crack propagation and delamination because of the macroscopic size of the crack tip. Many studies and standardization documents have proposed the use of a mark, scale, magnifying grass, and microscope to distinguish the position of the crack tip. [21–24] However, there are difficulties associated with this method; hence, an alternative method for accurate and easy identification of the position of the crack tip is required, so that the crack length and fracture toughness (G_{1c}) can be determined.

Here, we proposed a mechanoluminescence-assisted DCB test and demonstrate the effectiveness. Based on the mechanoluminescence, the appearance and movement of the crack tip was clearly visualized as the ML point along the adhesive layer on the side wall of the DCB specimen during crack propagation and delamination; then, the crack length was easily determined to obtain the fracture toughness. In addition, the formation and growth of cracks in bonded joints under mode I fracture was successfully visualized as a clear ML line on the top surface of the adherend of the DCB specimen.

Experimental

To demonstrate the effectiveness of the mechanoluminescence-assisted DCB test, a simple DCB specimen was prepared using sandblasted aluminum as the adherend and epoxy adhesive (Denatite 2204, Nagase ChemteX Co., Osaka, Japan; curing temperature: 100°C; thickness: ~100 μm), as shown in Figure 2(a). As the core part of the ML sensor, green-emitting europium-doped strontium aluminate ($SrAl_2O_4$:Eu^{2+}, denoted as SAOE, λ_{em} = 520 nm) was used because it shows the highest mechanoluminescence among a series of ML materials, with various emission colors across the ultraviolet to the infrared region. [3] Details on the preparation of the green-emissive SAOE microparticles (1 – 5 μm) by solid-phase have been described elsewhere. [1–3] ML sensors are of two types: paints and sheets. [3] Here, a commercial ML paint (ML-32ET, Sakai Chemical. Japan) was intentionally used for widely spreading in the field of structural adhesion. The ML paint was sprayed on the top and side surfaces of the DCB specimen to obtain ML films, as shown in Figure 2(b). From the microscopic images in Figure 2(c), the thickness of the ML films was estimated to be approximately 150 μm on the top surface and 100 μm on the side surface. The appropriate range of thickness values was used for visualizing the crack propagation and/or strain distribution.[3]

The conditions for the DCB test were identical to those for the conventional and original DCB test, except for the mechanoluminescence, as shown in Figure 3. Concretely, a tensional load at the rate of 1 mm/min was applied to the edge of the DCB specimen through a specific Jig, using a testing machine (A & D Co.) to generate mode I fracture and delamination at the adhesive layer (Sample number: 5). To record the mechanoluminescence in real time, two charge coupled device (CCD) cameras were used for obtaining the side and top images of the DCB specimen (CCD cameras **1** and **2** in Figure 3(a)). Delamination of the DCB specimens occurred during cohesive fracture, as shown in Figure 3(b). All ML measurements were carried out under dark conditions and at room temperature. For quantitative ML measurements, a tensile load was applied immediately after irradiation by blue light (λ = 470 nm) for 1 min.
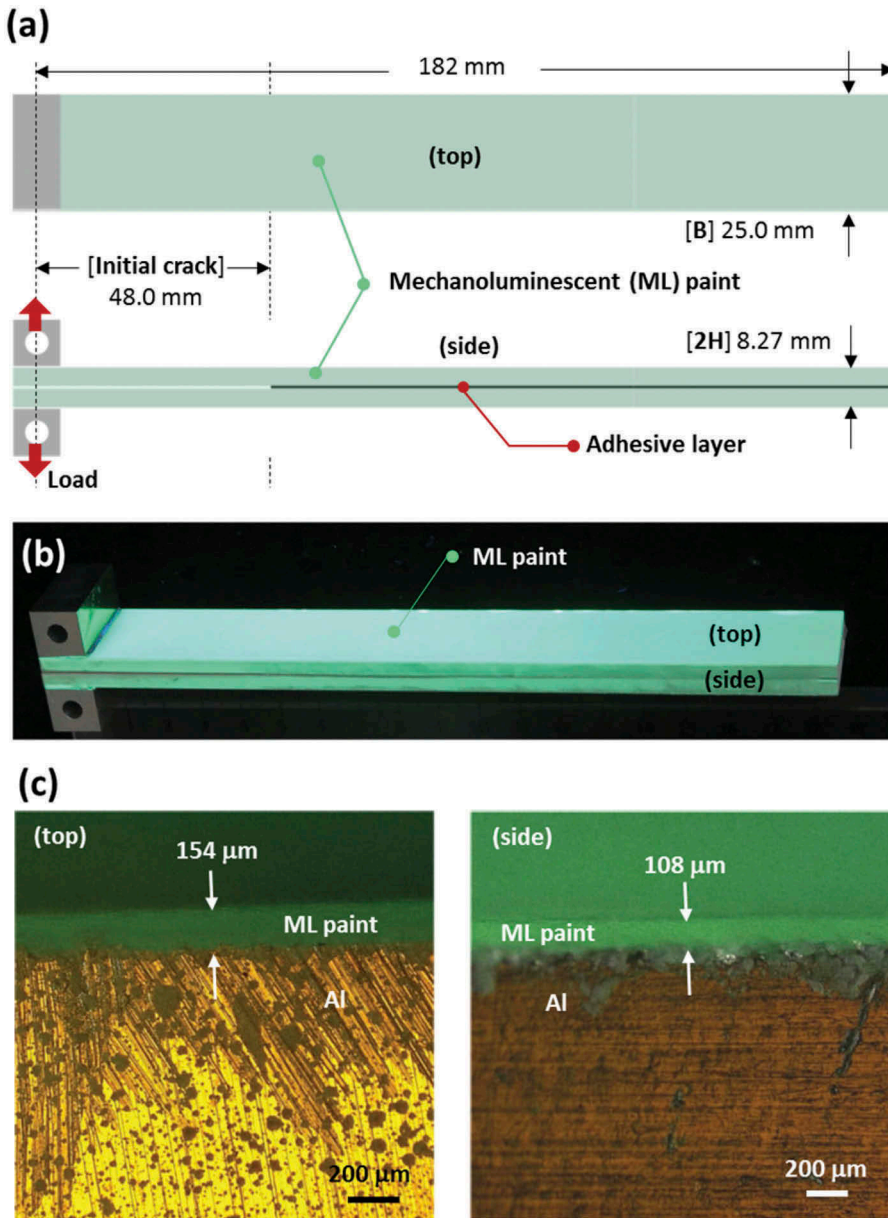
Figure 2. Mechanoluminescent (ML) paint-sprayed DCB specimen. (a) Illustration with sample information, (b) photograph, and (c) microscopic images of ML film sprayed on the top and side of the specimen under irradiation by excitation light (λ = 365 nm, 0.7 mW/cm^2).

Results and discussion

Figure 4 shows the mechanoluminescence results from the side images obtained using CCD camera **1** during the DCB test. At 100 s after loading, an intense mechanoluminescence emission point (ML point) gradually appeared at the position of the adhesive layer owing to strain concentration and fracture of the
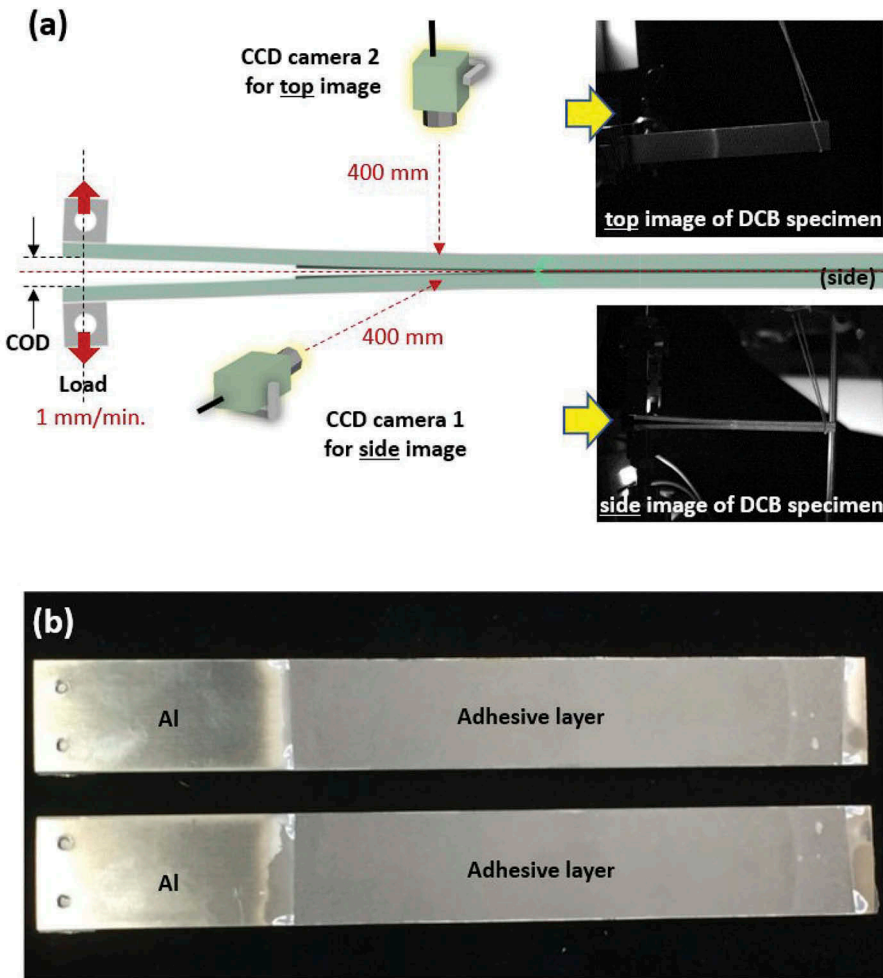
Figure 3. Experimental information. (a) Setup for mechanoluminescence-assisted DCB test and (b) photo of specimen after fracture.

adhesive layer and the ML film. Upon further tensile load application and following mode I fracture, i.e., crack propagation and delamination along the adhesive layer, the ML point smoothly moved from the initial crack tip to the end of the DCB specimen, as shown by the arrow marks in Figure 4.

From the ML images in Figure 4, an enlarged ML image was extracted, as shown in Figure 5(a), and the ML behavior during the DCB test was explained based on 3 observations. First, at the initial stage of fracture generation, strong mechanoluminescence was observed at the tip of the initial crack (mark **i**) owing to intense stress concentration. Then, as described above, moving of the ML point (mark **ii**) was observed along the adhesive layer during crack propagation and delamination in the DCB test. In addition to the ML point, an ML distribution was observed on the upper and lower adherends, slightly ahead of the ML point, due to
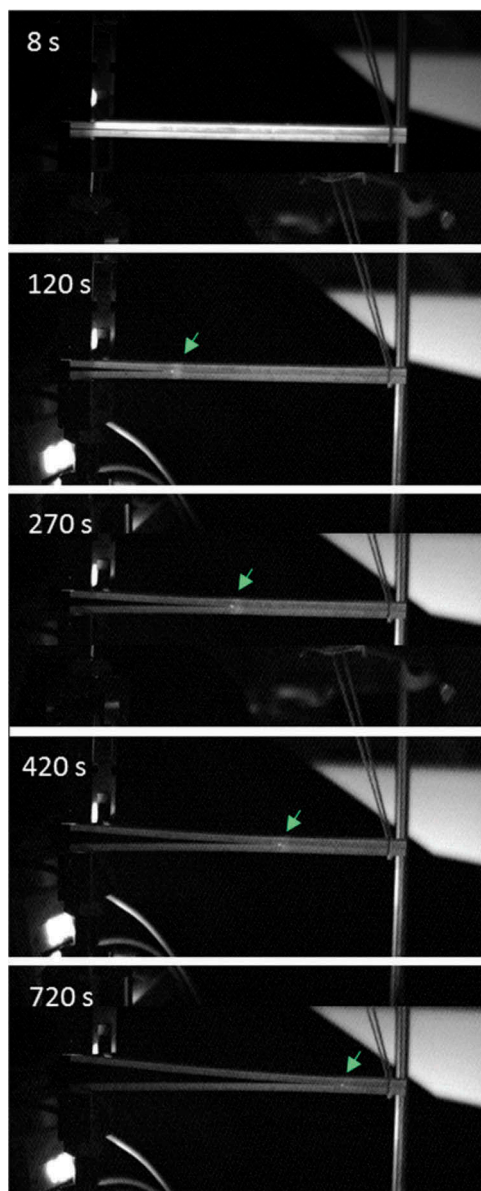
Figure 4. Mechanoluminescence results from side images of DCB specimen from CCD camera **1** during the test.

stress concentration at the crack tip accompanied with crack opening and bending, as shown at mark **iii**. From the sequence of ML images, the region of interest (denoted as ROI) was set for each ML point, and then, the ML points were automatically tracked by image processing software, as shown in Figure 5(b).

In Figure 6, the load value (N) and crack length (mm) were plotted as functions of the crack opening displacement (COD). The load and COD were derived from the testing machine, and the length was calculated from the
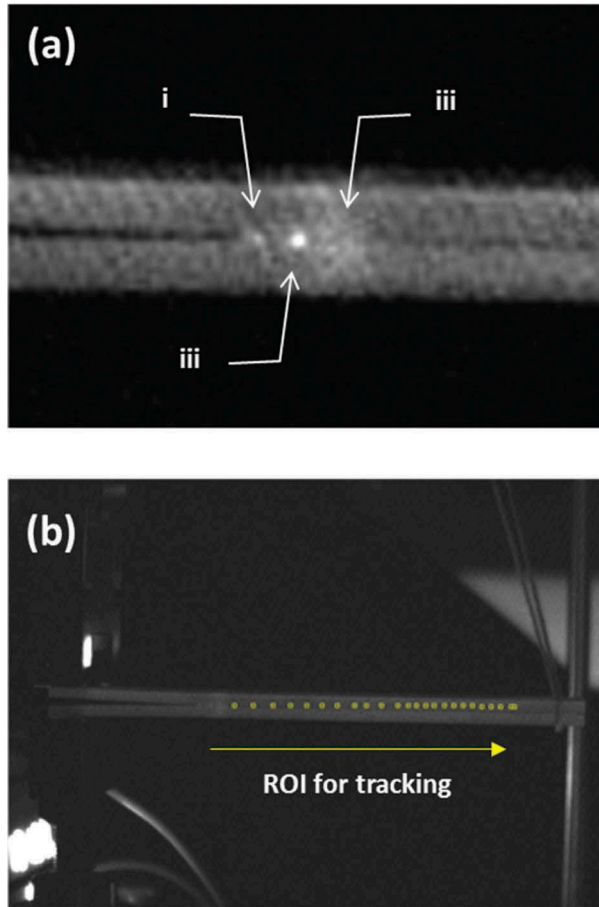
Figure 5. (a) Emphasizing point in mechanoluminescence results in Figure 5, (b) ROI for tracking ML points.

distance between the initial crack tip and the ML points tracked by the ROI. At around 100 s after loading, the load reached the maximum value and the time was synchronized to the time when the ML point started moving. This result supported the fact that the ML point reflects the crack tip accompanied by fracture, crack propagation, and delamination of the DCB specimen. By using these experimental values, sample values, and Equation 1 [21–24], the fracture toughness G_{1c} (kJ/m^2) was successfully calculated, as shown in Figure 7(b).

$$G_{1c} = \frac{3}{4H} \left(\frac{Pc}{B}\right)^2 \frac{(B\lambda)^{\frac{2}{3}}}{\alpha_1} \tag{1}$$

where *2H* is the thickness (mm) of the DCB specimen, *Pc* is the load (N), B is the width of the specimen, λ is the COD compliance (mm/N), and α_1 is obtained as the slope of (a/2H) and $(B/\lambda)^{1/3}$.
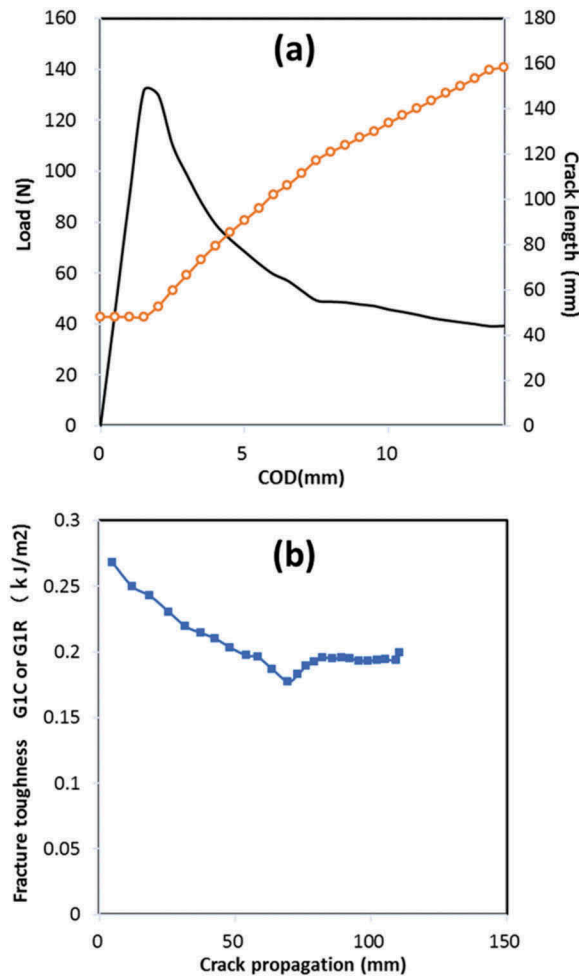
Figure 6. Time course of (a) load and crack length against crack opening displacement (COD) and (b) fracture toughness.

In order to demonstrate the accuracy of the new method to distinguish the crack tip using mechanoluminescence, microscopic observations were carried out on the side wall of the specimen during the mechanoluminescence-assisted DCB test, as shown in Figure 7(a). Upon load application and the subsequent crack initiation and propagation, the brightness of the area responding to the pre-crack tip increased continuously (Figure 7(b)), and this area and the ML point gradually moved to the right (Figure 7(c–e)). Notably, as shown in Figure 7(c–e), the point with the highest mechanoluminescence could be observed just 0–20 μm ahead of the crack tip. This result clearly demonstrated that mechanoluminescence accurately reflects the position of the crack tip, even on the microscopic scale. In addition, intense mechanoluminescence could be observed 0–300 μm ahead of the crack tip, probably because of the effect of microcracks in the process zone. [25]
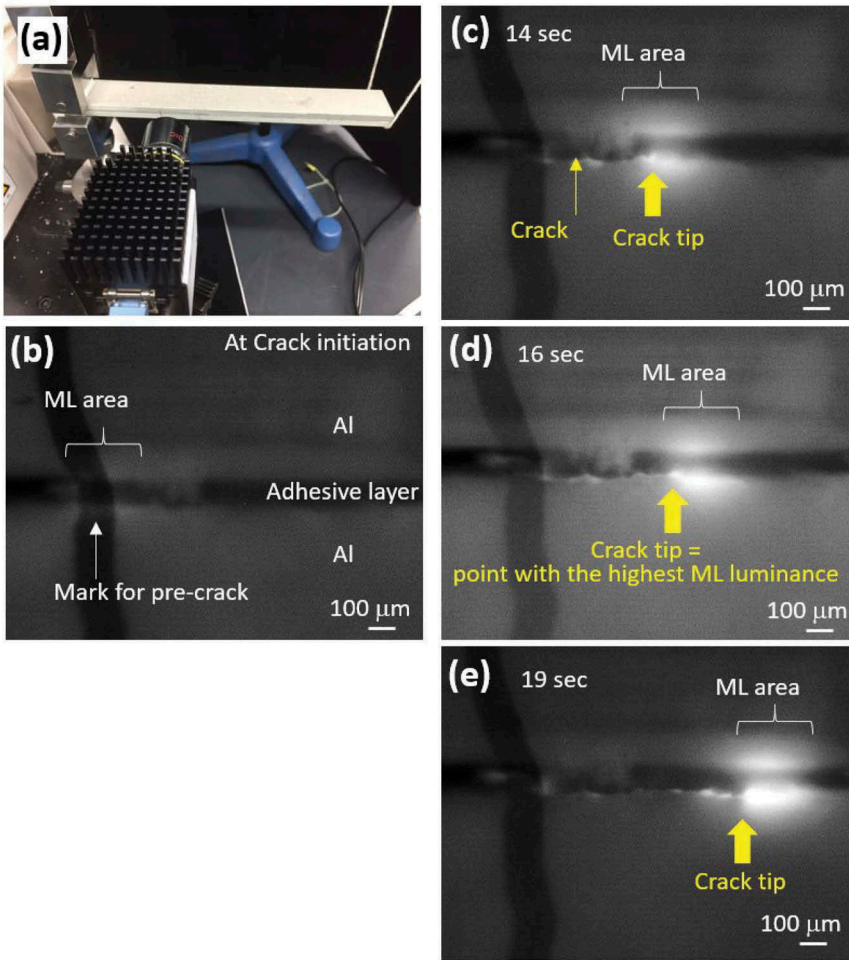
Figure 7. Mechanoluminescence result for the side of the DCB specimen using a microscopic measurement system. (a) Setup, (b) ML images recorded at 0, 14, 16, and 19 s after crack initiation.

The results of the DCB test in the side view revealed that the fracture points could always be distinguished easily by the clear and intense mechanoluminescence during the entire testing period. Therefore, it can be concluded that ML sensing has high potential in assisting conventional and important DCB tests and analyses, especially for detecting the crack tip.

Figure 8 shows the mechanoluminescence results for the top images obtained by CCD camera **2** during the DCB test. Upon load application and COD, an ML line gradually appeared in perpendicular orientation to the adhesive frontline at the position of the initial crack tip until 100 s of loading (time of maximum loading). Then, an intense ML line moved synchronous with the crack tip, slightly ahead of the tip, as visualized by the
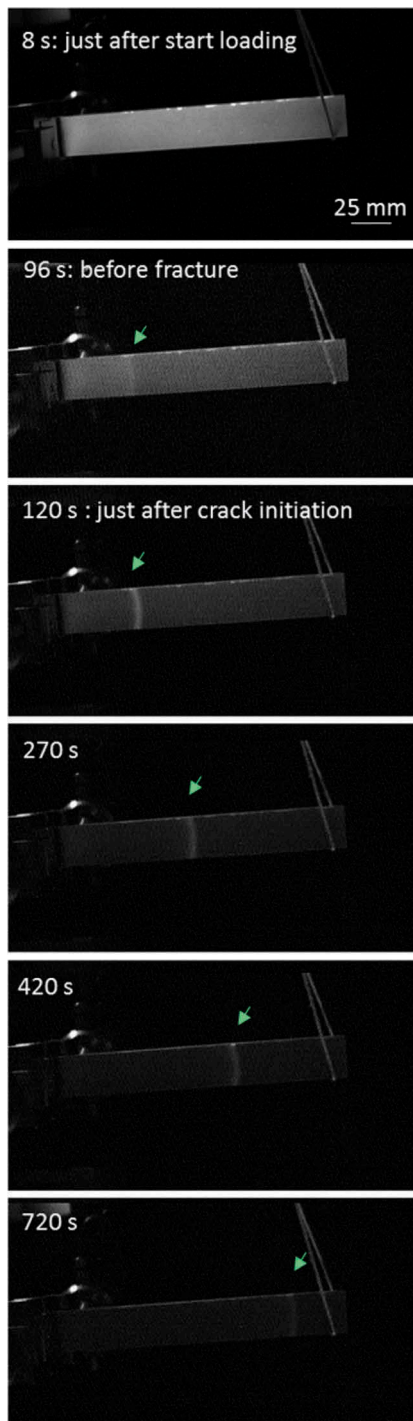
Figure 8. Mechanoluminescence result from top images of the DCB specimen obtained using CCD camera **2** during the test.

mechanoluminescence on the side of the specimen. The width of the ML line was estimated as 2–3 mm, and the position of the line was slightly ahead the crack tip, with an intense ML point in side view. This result could be supported by the observations reported by Budzik and co-workers on substrate deflection in the crack vicinity. [25] Interestingly, the ML line was almost straight before fracture initiation and then became slightly curved at the steady state of crack propagation. Here, the ML line originated from strain concentration owing to elastic bending deformation of the aluminum adherend with the crack opening displacement and adhesive frontline as a balance point. In other words, the ML line probably reflects (1) the shape of the adhesive frontline as the balance point for strain concentration in the adherend and (2) the fracture toughness of each point in the line under mode I fracture. Originally, the crack length was determined using the average of crack length measured on both sides, with the assumption that the adhesive frontline is straight, because the real crack length at the center of the DCB specimen was undetectable in real-time DCB tests. In the original DCB tests, we had no choice but to consider the average fracture toughness for one adhesive frontline. However, it is important to distinguish a specific point and area in adhesive strengthen and fracture toughness owing to surface treatment condition, contamination, curing condition and so on. This successfully demonstrated that the mechanoluminescence sensing is not only effective for assisting the original DCB test but also provides useful additional information such as the cause of fracture toughness distribution in the DCB test.

Conclusion

Here, we proposed a mechanoluminescence-assisted DCB test. Through mechanoluminescence, a crack tip was clearly visualized and tracked during crack propagation in the DCB test, thus overcoming the difficulty in detecting tiny crack tips, and the crack length was easily determined to obtain the fracture toughness. This demonstrates the effectiveness of mechanoluminescence as a powerful assisting tool in the DCB test. In addition, mechanoluminescence sensing using the top image of the DCB specimen successfully provided useful information regarding the fracture and adhesive frontline to visualize the distribution of fracture toughness and adhesive strength in the DCB test. In the present case, we used a similar material joint of aluminum, and the ML line was rather straight and the moving was smooth and steady. However, in the case of the dissimilar material joint sample, the mechanoluminescence results from the top image would be more important to understand the fracture behavior reflecting the surface conditions and adhesion. In addition, the DCB test in modes II and III must provide important information, similar to that in mode I here. Thus, our investigation will continue along this strategy.

Acknowledgement

References

[1] Xu, C. N.; Watanabe, T.; Akiyama, M.; Zheng, X. G. Direct View of Stress Distribution in Solid by Mechanoluminescence. *Appl. Phys. Lett.* 1999, *74*, 2414–2417. DOI: 10.1063/1.123865.

[2] Li, C.; Xu, C. N.; Zhang, L.; Yamada, H.; Imai, Y. Dynamic Visualization of Stress Distribution on Metal by Mechanoluminescence Images. *J. Visualization.* 2008, *11*, 329–335. DOI: 10.1007/BF03182201.

[3] Xu, C. N.; Ueno, N.; Terasaki, N.; Yamada, H. *Mechanoluminescence and Novel Structural Health Diagnosis*; book style, Tokyo: NTS, 2012.

[4] Terasaki, N.; Xu, C. N. *Jpn. J. Appl. Phys.* 2009, *49*, 04C150-1-04C150-4.

[5] Terasaki, N.; Xu, C. N.; Li, C.; Zhang, L.; Li, C. Z.; Ono, D.; Tsubai, M.; Adachi, Y.; Imai, Y.; Ueno, N.; Shinokawa, T. *Proc. SPIE SMART STRUCTURES/NDE.* 2012, *2*, 8348D1–8348D6.

[6] Terasaki, N.; Xu, C. N.; Yasuda, K.; Ichinose, L. *Proc. 6th Int. Conf. Bridge Maintenance, Saf. Manag.* 2012, *6*, 2542–2549.

[7] Terasaki, N.; Xu, C. N. Historical-Log Recording System for Crack Opening and Growth Based on Mechanoluminescent Flexible Sensor. *IEEE Sens. J.* 2013, *13*, 3999–4004. DOI: 10.1109/JSEN.2013.2264665.

[8] Terasaki, N.; Li, C.; Zhang, L.; Xu, C. N. *IEEE Sensors Appl. Symp. Proc.* 2012, *2012*, 77–81.

[9] Fujio, Y.; Xu, C. N.; Terasawa, Y.; Sakata, Y.; Yamabe, J.; Ueno, N.; Terasaki, N.; Yoshida, A.; Watanabe, S.; Murakami, Y. Sheet Sensor Using SrAl 2 O 4 :Eu Mechanoluminescent Material for Visualizing Inner Crack of High-Pressure Hydrogen Vessel. *Int. J. Hydrogen Energy.* 2015, *41*, 1333–1340. DOI: 10.1016/j.ijhydene.2015.10.073.

[10] Terasaki, N.; Fujio, Y.; Sakata, Y.; Uehara, M.; Tabaru, T. Direct Visualization of Stress Distribution Related to Adhesive through Mechanoluminescence. *ECS Trans.* 2017, *75*, 9–16. DOI: 10.1149/07545.0009ecst.

[11] Terasaki, N.; Fujio, Y.; Sakata, Y. *Proc. 29th Int. Committee Aeronau. Fatigue Struct. Integrity (ICAF2017) Symp.* 2017, *75*, 1961–1967.

[12] Da Silva, L. F. M. D.; Öchsner, A.; Adams, R. *Handbook of Adhesion Technology*; Berlin: Springer, 2011.

[13] Ishai, O.; Rosenthal, H.; Sela, N.; Drukker, E. Effect of Selective Adhesive Interleaving on Interlaminar Fracture Toughness of Graphite/Epoxy Composite Laminates. *Composites.* 1988, *19*, 49–54. DOI: 10.1016/0010-4361(88)90543-5.

[14] Bane, A. M. D.; Da Silva, L. F. M. D.; Campilho, R. D. S. G. *J. Adhes. Sci. Technol.* 2012, *26*, 939–953.

[15] Chen, Z.; Adams, R.; Silva, D.; L. F., M. D. Fracture Toughness of Bulk Adhesives in Mode I and Mode III and Curing Effect. *Int. J. Fract.* 2011, *167*, 221–234. DOI: 10.1007/s10704-010-9547-9.

[16] Richter -Trummer, M.; Chaves, E. A.; Tavares, F. J. P.; Da Silva, J. M. R. S.; L. F. M.,; De Castro, P. M. S. T. *Materwiss Werksttech.* 2011, *42*, 452–459. DOI: 10.1002/mawe.201100807.

[17] Chaves, F. J. P.; Silva, L. F. M. D.; Moura, M. F. S. F. D.; Dillard, D. A.; Esteves., V. H. C. Fracture Mechanics Tests in Adhesively Bonded Joints: A Literature Review. *J. Adhes.* 2014, *90*, 955–992. DOI: 10.1080/00218464.2013.859075.

[18] Moura, M. F. S. F.; Gonçalves, J. P. M.; Magalhães, A. G. A Straightforward Method to Obtain the Cohesive Laws of Bonded Joints under Mode I Loading. *Int. J. Adhes. Adhes.* 2012, *39*, 54–59. DOI: 10.1016/j.ijadhadh.2012.07.008.

[19] Salem, N. B.; Budzik, M. K.; Jumel, J.; Shanahan, M. E. R.; Lavelle, F. Investigation of the Crack Front Process Zone in the Double Cantilever Beam Test with Backface Strain Monitoring Technique. *Eng. Fract. Mech.* 2013, *98*, 272–283. DOI: 10.1016/j.engfracmech.2012.09.028.

[20] Sarrado, C.; Turon, A.; Costa, J.; Renart, J. On the Validity of Linear Elastic Fracture Mechanics Methods to Measure the Fracture Toughness of Adhesive Joints. *Int. J. Solids Struct.* 2016, *81*, 110–116. DOI: 10.1016/j.ijsolstr.2015.11.016.

[21] Standardization Documents. For Example, (A) ISO 25217 "Adhesives – Determination of the Mode 1 Adhesive Fracture Energy of Structural Adhesive Joints Using Double Cantilever Beam and Tapered Double Cantilever Beam Specimens", (B) ASTM D5528-13 "Standard Test Method for Mode I Interlaminar Fracture Toughness of Unidirectional Fiber-Reinforced Polymer Matrix Composites", (C) JIS K7086 "Testing Methods for Interlaminar Fracture Toughness of Carbon Fiber Reinforced Plastics", (D) ISO 15024 " Fiber-Reinforced Plastic Composites – Determination of Mode I Interlaminar Fracture Toughness, G_{IC}, for Unidirectionally Reinforced Materials" Etc.

[22] O'Brien, T. K.;. Interlaminar Fracture Toughness: The Long and Winding Road to Standardization. *Composites Part B.* 1998, *298*, 57–62. DOI: 10.1016/S1359-8368(97)00013-9.

[23] Horiuchi, S.; Hakukawa, H.; Kim, N. Y. J.; Sugimura, H. Study of the Adhesion and Interface of the Low-Temperature Bonding of Vacuum Ultraviolet-Irradiated Cyclo-Olefin Polymer Using Electron Microscopy. *Polymer J.* 2016, *48*, 473–479. DOI: 10.1038/pj.2016.3.

[24] Ye, L.;. Evaluation of Mode-I Interlaminar Fracture Toughness for Fiber-Reinforced Composite Materials. *Composites Sci. Technol.* 1992, *43*, 49–54. DOI: 10.1016/0266-3538(92)90132-M.

[25] Budzik, M. K.; Jumel, J.; Shanahan, M. E. R. Formation and Growth of the Crack in Bonded Joints under Mode I Fracture: Substrate Deflection at Crack Vicinity. *J. Adhesion.* 2011, *87*, 967–988. DOI: 10.1080/00218464.2011.609441.